General Disclaimer

One or more of the Following Statements may affect this Document

- This document has been reproduced from the best copy furnished by the organizational source. It is being released in the interest of making available as much information as possible.

- This document may contain data, which exceeds the sheet parameters. It was furnished in this condition by the organizational source and is the best copy available.

- This document may contain tone-on-tone or color graphs, charts and/or pictures, which have been reproduced in black and white.

- This document is paginated as submitted by the original source.

- Portions of this document are not fully legible due to the historical nature of some of the material. However, it is the best reproduction available from the original submission.

X-622-76-75
PREPRINT

NASA TM X-71111

INFLUENCE OF PLANETARY-SCALE TOPOGRAPHY ON THE DIURNAL THERMAL TIDE DURING THE 1971 MARTIAN DUST STORM

BARNEY J. CONRATH

JANUARY 1976

GSFC — GODDARD SPACE FLIGHT CENTER —
GREENBELT, MARYLAND

INFLUENCE OF PLANETARY - SCALE TOPOGRAPHY ON THE DIURNAL THERMAL TIDE DURING THE 1971 MARTIAN DUST STORM

Barney J. Conrath
Laboratory for Planetary Atmospheres

January 1976

GODDARD SPACE FLIGHT CENTER
Greenbelt, Maryland 20771

ABSTRACT

Data obtained with the Mariner 9 infrared spectroscopy experiment during the Martian Dust Storm of 1971-72 are examined for evidence of topographic influence on the atmospheric thermal structure. Temperature perturbations which are well correlated with the planetary scale topography are found superposed on the large amplitude diurnal thermal tide previously reported. Applications of tidal theory to the data indicate that the observed perturbations result from the kinematic interaction of the westward traveling diurnal wave with the large scale components of topography. The dominant mode is excited by the wave-number two topography component and is a vertically evanescent eastward traveling wave with an equivalent depth comparable to the atmospheric scale height. The principle dynamic effect of this mode is the enhancement of the amplitude of the near-surface diurnal wind to over 40 m s^{-1} in limited areas near 30° south latitude. Thus, it appears likely that dust was injected into the atmosphere in these regions during the storm. Other waves excited include vertically propagating modes which produce little effect in the lower atmosphere, but may represent a source of energy for the upper atmosphere during dust storm conditions.

Introduction

The Mariner 9 spacecraft was injected into orbit about Mars on 14 November 1971 during a major planet-wide dust storm. Extensive data were acquired during the storm and its subsequent decay. Analyses of these data have provided information on the physical and dynamical state of the atmosphere during the storm. The dust cloud which extended to a height of ~50 km (Leovy, et al. 1972) was found to exert a profound influence on the thermal structure of the atmosphere (Hanel, et al., 1972; Kliore, et al., 1972). Atmospheric temperatures obtained with the Mariner 9 infrared spectroscopy experiment (IRIS) indicated mean temperatures substantially higher than those expected for a clear CO_2 atmosphere. A diurnal temperature wave was found with a peak-to-peak amplitude approaching 30K at some latitudes extending from the surface to at least 40km (Hanel, et al., 1972; Conrath, et al., 1973).

Temperature data obtained during the dust storm have been used to study the thermally driven atmospheric tidal system (Leovy, et al., 1973; Pirraglia and Conrath, 1974). In these studies, the surface of the planet was assumed to be a smooth sphere. However, it is known from a variety of measurements that the surface of Mars possesses substantial topographic relief on both a local and planetary scale (see for example Downs, et al., 1975; Kliore, et al., 1972; Hord et al., 1974; Conrath, et al., 1973). This relief can locally reach or exceed an atmospheric scale height. Lindzen (1970) has pointed out that the atmospheric tidal waves can interact with the large scale topography to produce perturbations

on the Martian tidal regime, and Zurek (1976) has considered this problem in some detail. It is the purpose of the present study to examine the Mariner 9 IRIS temperature data for evidence of the existence of effects related to the large scale topographic relief.

First the IRIS temperature data will be analyzed and correlated with topography. Next a first order model of the modulation of the tidal waves by large scale topography will be developed. Finally the theoretical results will be compared with the observational data, and conclusions will be drawn concerning the effectiveness of the large scale topography in modifying the tidal structure.

Data Analysis

Temperature profiles were reconstructed from the IRIS data using measurements in selected spectral intervals within the 667 cm^{-1} CO_2 absorption band. The analytical methods employed are similar to those developed for use in the terrestrial meteorological satellite program (see for example Conrath and Revah, 1972). The vertical resolution of the retrieved profiles is about one-half of an atmospheric scale height and the RMS random error due to instrumental noise is estimated to be 2-3K. Useful information is obtained from the planetary surface up to about the 0.1 mb level.

Temperature at the 2 mb level of the atmosphere is plotted versus longitude for three different latitude intervals in Figures 1, 2, and 3. Each data point is taken from an individual temperature sounding. The data were obtained during

the first 47 days of the Mariner 9 mission and are shown for both morning and evening conditions. At the bottom of each figure, the mean surface elevation is given for the latitude interval 0° to -45° for purposes of comparison. These data were also obtained from the IRIS experiment using measurements in the wing of the 667 cm^{-1} CO_2 band (J. Pearl private communication, 1975). In both the early morning and late afternoon, there is an apparent correlation with topography. The atmosphere is warmer over depressions and cooler over higher elevations in the morning. In the late afternoon, the situation is reversed with warmer temperatures occuring over higher elevations and cooler temperatures over lower regions. The mid-day data coverage is much less complete and a detailed analysis cannot be made during the local time intervals from mid-morning to early afternoon.

One possibility for the observed temperature behavior is the modulation of the thermal tide by the large scale topography. To persue this possibility further, it is necessary to first consider the theory of topographic interaction with the tidal wave.

Theory

Chapman and Lindzen (1970) have given a qualitative discussion of the general problem of the interaction of tides with the planetary surface, demonstrating that waves may occur with phase speeds different from that of the solar excitation, and Zurek (1976) has developed a computational method for treating

the complete tidal problem. For purposes of interpreting the data considered here, however, a simplified theoretical model will be developed. The approach taken is as follows. The amplitude of the diurnal temperature wave can be regarded as consisting of a zonal mean plus a longitudinally varying component. The zonal mean will be used, along with the observed planetary-scale topography, to calculate the longitude dependent component. A comparison can then be made with the observed longitudinal variations.

The theory of the thermally driven atmospheric tide on a smooth spherical planet has been reviewed in detail by Chapman and Lindzen; for a discussion of the basic assumptions involved and the detailed mathematical development, the reader is referred to their work. The basic independent variable normally employed in atmospheric tidal theory is

$$G = -\frac{1}{\gamma p_0}\frac{Dp}{Dt} \tag{1}$$

where p is atmospheric pressure, p_0 is atmospheric pressure for the unperturbed (static) state, and γ is the ratio of specific heats. If it is assumed that J, the thermotidal heating per unit mass per unit time, can be written

$$J(\theta, \phi, z, t) = J^{\sigma, s_0}(\theta, Z)\, e^{i(s_0\phi + \sigma t)} \tag{2}$$

and that

$$G(\theta, \phi, Z, t) = G^{\sigma}(\theta, \phi, Z)\, e^{i\sigma t}, \tag{3}$$

then it can be shown that G^σ must satisfy

$$H\frac{\partial^2 G^\sigma}{\partial Z^2} - \frac{\partial G^\sigma}{\partial Z} = \frac{g}{4a^2\Omega^2}\,\mathfrak{H}\left(\kappa G^\sigma - \frac{\kappa}{\gamma g H}\,J^{\sigma, s_0}\,e^{i s_0 \phi}\right). \tag{4}$$

The operator $\mathfrak{H}$ is defined as

$$\mathfrak{H} = \frac{1}{\sin\theta}\,\frac{\partial}{\partial\theta}\left(\frac{\sin\theta}{f^2 - \cos^2\theta}\,\frac{\partial}{\partial\theta}\right) + \frac{1}{f^2 - \cos^2\theta}\left(\frac{i}{f}\,\frac{f^2 + \cos^2\theta}{f^2 - \cos^2\theta}\,\frac{\partial}{\partial\phi} + \frac{1}{\sin^2\theta}\,\frac{\partial^2}{\partial\phi^2}\right). \tag{5}$$

The notation is as follows:

θ = colatitude

ϕ = east longitude

σ = wave frequency

s_0 = longitudinal wavenumber of source of excitation

Z = vertical height

H = scale height

a = radius of planet (=3383 km)

Ω = siderial rotation rate of planet ($=7.09003 \times 10^{-5}$ $\sec^{-1}$)

g = gravitational acceleration (=370 cm $\sec^{-2}$)

κ = R/C_p (=0.23)

R = gas constant ($=1.89 \times 10^{-6}$ ergs gm^{-1} deg^{-1})

C_p = specific heat at constant pressure ($=8.22 \times 10^{-6}$ ergs gm^{-1} deg^{-1})

f = $\sigma/2\Omega$

For a diurnal wave with a period of one mean solar day, $\sigma = 7.07765 \times 10^{-5}$ sec^{-1}. The scale height H will be taken as constant in all subsequent calculations, and the values used for the thermodynamic parameters are for a pure CO_2 atmosphere.

With the specification of appropriate boundary conditions, (4) can be solved for G from which the other tidal field variables can be obtained. In addition to the requirement that the solution be finite at the poles, boundary conditions must be specified at the planetary surface and for $z \to \infty$. The upper boundary condition will be discussed later. The lower boundary condition for a smooth spherical planet is usually taken as $w(z = 0) = 0$ where w is the vertical tidal velocity. In the presence of topography, this condition must be generalized to the requirement that the component of tidal velocity locally normal to the surface must vanish. If $\xi(\theta, \phi)$ represents the surface elevation above a reference surface of constant geopotential, this condition can be written approximately as

$$w = \mathbf{v} \cdot \nabla \xi \quad \text{at} \quad z = 0 \tag{6}$$

where $\mathbf{v}$ is the horizontal velocity field and ∇ is the horizontal gradient operator.

Consider now a component of topography with longitudinal wave number m written in the form

$$\xi(\theta, \phi) = \xi_m(\theta) \cos(m\phi + \delta_m). \tag{7}$$

Let the following definitions be introduced:

$$\epsilon a_m = \frac{1}{2} \frac{im}{\sin\theta} \frac{\xi_m}{H} e^{i\delta_m}$$

$$\epsilon b_m = \frac{1}{2} \frac{\partial}{\partial\theta}\left(\frac{\xi_m}{H}\right) e^{i\delta_m}$$

$$a_{-m}(\theta) = a_m^*(\theta)$$

$$b_{-m}(\theta) = b_m^*(\theta)$$

where the asterisks denote complex conjugation, and $\epsilon = \max \xi_m / H$. Introduction of (7) into (6) gives the appropriate lower boundary condition

$$w(0) = \epsilon \frac{H}{a} \{[b_m(\theta)\, u(0) + a_m(\theta)\, v(0)]\, e^{im\phi} + [b_{-m}(\theta)\, u(0) + a_{-m}(\theta)\, v(0)]\, e^{-im\phi}\} \tag{8}$$

where u is the southward component of tidal velocity and v is the eastward component.

If it is assumed the a_m and b_m are of order unity and $\epsilon << 1$, then a separable problem can be obtained by expanding G^σ, u^σ, and v^σ in powers of ϵ, i.e.,

$$G^\sigma = G_0^\sigma + \epsilon G_1^\sigma + \epsilon^2 G_2^\sigma + \cdots \tag{9}$$

$$u^\sigma = u_0^\sigma + \epsilon u_1^\sigma + \epsilon^2 u_2^\sigma + \cdots \tag{10}$$

$$v^\sigma = v_0^\sigma + \epsilon v_1^\sigma + \epsilon^2 v_2^\sigma + \cdots \tag{11}$$

Substituting (8) into (4) and equating like powers of ϵ yields an infinite set of differential equations. The zero order and first order equations are

$$\frac{\partial^2 G_0^\sigma}{\partial x^2} - \frac{\partial G_0^\sigma}{\partial x} = \frac{gH}{4a^2\Omega^2}\, \mathfrak{F}\left(\kappa G_0^\sigma - \frac{\kappa}{\gamma gH}\, J^{\sigma, s_0}\, e^{is_0\phi}\right) \tag{12}$$

and

$$\frac{\partial^2 G_1^\sigma}{\partial x^2} - \frac{\partial G_1^\sigma}{\partial x} = \frac{gH}{4a^2\Omega^2}\, \mathfrak{F}(\kappa G_1^\sigma) \tag{13}$$

where $x = z/H$. In a similar fashion, substitution of (10) and (11) into (8) gives the corresponding lower boundary conditions

$$w_0^\sigma(\theta, \phi, 0) = 0 \tag{14}$$

and

$$w_1^\sigma(\theta, \phi, 0) = \frac{H}{a}\, [a_m(\theta)\, v_0^\sigma(\theta, \phi, 0) + b_m(\theta)\, u_0^\sigma(\theta, \phi, 0)]\, e^{im\phi}$$

$$+ \frac{H}{a}\, [a_{-m}(\theta)\, v_0^\sigma(\theta, \phi, 0) + b_{-m}(\theta)\, u_0^\sigma(\theta, \phi, 0)]\, e^{-im\phi}. \tag{15}$$

Considering first the zero order tidal equation (12), separation of variables is accomplished by assuming

$$J^{\sigma,s_0}(\theta, x) = \sum_n J_n^{\sigma,s_0}(x)\, \Theta_n^{\sigma,s_0}(\theta) \tag{16}$$

$$G_0^{\sigma}(\theta, \phi, x) = \sum_n e^{x/2}\, y_n^{\sigma,s_0}(x)\, \Theta_n^{\sigma,s_0}(\theta)\, e^{is_0\phi} \tag{17}$$

where the functions $\Theta_n^{\sigma,s}$ satisfy the eigenvalue equation

$$\left[\frac{1}{\sin\theta}\frac{\partial}{\partial\theta}\left(\frac{\sin\theta}{f^2-\cos^2\theta}\frac{\partial}{\partial\theta}\right) - \frac{1}{f^2-\cos^2\theta}\left(\frac{s}{f}\frac{f^2+\cos^2\theta}{f^2-\cos^2\theta}\right) + \frac{s^2}{\sin^2\theta}\right]\Theta_n^{\sigma,s}$$

$$= -\frac{4a^2\Omega^2}{gh_n^{\sigma,s}}\Theta_n^{\sigma,s}, \tag{18}$$

and the height dependent factors are obtained from the vertical structure equation

$$\frac{d^2y_n^{\sigma,s_0}}{dx^2} + \left(\kappa\frac{H}{h_n^{\sigma,s_0}} - \frac{1}{4}\right)y_n^{\sigma,s_0} = \frac{\kappa}{\gamma gh_n^{\sigma,s_0}}J_n^{\sigma,s_0}e^{-x/2}. \tag{19}$$

Equation (18) is Laplace's Tidal Equation, and the eigenfunctions $\Theta_n^{\sigma,s}$ are known as Hough functions. They can be represented as infinite series of associated Legendre functions, and their properties have been extensively discussed in the literature. The eigenvalues are here written in the conventional form $-4a^2\Omega^2/gh_n^{\sigma,s_0}$ where h_n^{σ,s_0} is the so-called equivalent depth.

The tidal fields which are of interest for the present discussion can be written

$$\delta p = \sum_n \delta p_n(x)\, \Theta_n(\theta) \tag{20}$$

$$\delta T = \sum_n \delta T_n(x)\, \Theta_n(\theta) \tag{21}$$

$$u = \sum_n u_n(x)\, U_n(\theta) \tag{22}$$

$$v = \sum_n v_n(x)\, V_n(\theta) \tag{23}$$

$$w = \sum_n w_n(x)\, \Theta_n(\theta) \tag{24}$$

where the superscripts σ ,s have been surpressed. δT and δp are the tidal temperature and pressure fluctuations. The functions U_n and V_n are related to Θ_n by

$$U_n = \frac{1}{f^2 - \cos^2\theta}\left(\frac{d}{d\theta} + \frac{s_0}{f}\cot\theta\right)\Theta_n(\theta), \tag{25}$$

$$V_n = \frac{1}{f^2 - \cos^2\theta}\left(\frac{\cos\theta}{f}\frac{d}{d\theta} + \frac{s_0}{\sin\theta}\right)\Theta_n(\theta). \tag{26}$$

The height dependent factors in (20)-(24) can be expressed in terms of solutions of the vertical structure equation (19):

$$\delta p_n(x) = p_0(0)\,\frac{\gamma}{i\sigma}\,\frac{h_n}{H}\,e^{-x/2}\left(\frac{dy_n}{dx} - \frac{1}{2}\,y_n\right), \tag{27}$$

$$\delta T_n(x) = \frac{\kappa}{i\sigma R}\,(J_n - \gamma g H e^{x/2} y_n), \tag{28}$$

$$u_n(x) = \frac{\gamma g h_n}{4a\Omega^2}\,e^{x/2}\left(\frac{dy_n}{dx} - \frac{1}{2}\,y_n\right), \tag{29}$$

$$v_n(x) = i\,u_n(x), \tag{30}$$

$$w_n(x) = \gamma h_n e^{x/2}\left[\frac{dy_n}{dx} + \left(\frac{H}{h_n} - \frac{1}{2}\right)y_n\right]. \tag{31}$$

Using (31), the zero order lower boundary condition (14) can be written

$$\frac{dy_n}{dx} + \left(\frac{H}{h_n} - \frac{1}{2}\right) y_n = 0 \quad \text{at } x = 0. \tag{32}$$

In the usual approach to the tidal problem, the J_n's are specified, and (19) is solved subject to (32) and an upper boundary condition. However, in the present problem, the temperature field can be directly specified from the observations. It is desired to take the zero order tidal temperature field as given, and calculate the perturbation fields due to interaction of the zero order fields with the topography. The zero order quantities which will be

required in obtaining the first order solution are $u_n(0)$ and $v_n(0)$, and from (29) and (32)

$$u_n^{\sigma,s_0}(0) = -\frac{\gamma g H}{4a\Omega^2} y_n^{\sigma,s_0}(0). \tag{33}$$

A relationship between $y_n^{\sigma,s_0}(0)$ and $\left\langle \delta T_n^{\sigma,s_0} \right\rangle$, the density weighted vertical average of the zero order tidal temperature component $\delta T_n^{\sigma,s_0}$, is derived in the Appendix. Using this result, (33) can be written

$$u_n^{\sigma,s_0}(0) = -\frac{i\sigma}{4a\Omega^2}\left(\frac{H/h_n^{\sigma,s_0}}{H/h_n^{\sigma,s_0} - 1}\right) R \left\langle \delta T_n^{\sigma,s_0} \right\rangle. \tag{34}$$

Solution of the first order equation (13) subject to the lower boundary condition (15) will now be considered. Let

$$G_1^{\sigma}(\theta, \phi, x) = \sum_s G^{\sigma,s}(\theta, x)\, e^{is\phi} \tag{35}$$

and substitute into (13). This yields a set of homogeneous equations of the form

$$\frac{\partial^2 G^{\sigma,s}}{\partial x^2} - \frac{\partial G^{\sigma,s}}{\partial x} - \frac{\kappa g H}{4a^2\Omega^2} F_s(G^{\sigma,s}) = 0 \tag{36}$$

where F_s is the differential operator in square brackets in the left hand side of (18) with s_0 replaced by s. If $G^{\sigma,s}$ is expanded in terms of $\Theta_n^{\sigma,s}$ where

$$F_s \Theta_n^{\sigma,s} = -\frac{4a^2\Omega^2}{gh_n^{\sigma,s}} \Theta_n^{\sigma,s}, \tag{37}$$

there results a set of homogeneous vertical structure equations

$$\frac{d^2 y_n^{\sigma,s}}{dx^2} + \left(\kappa \frac{H}{h_n^{\sigma,s}} - \frac{1}{4}\right) y_n^{\sigma,s} = 0. \tag{38}$$

The first order vertical velocity can be expanded in the form

$$w_1^{\sigma}(\theta, \phi, x) = \sum_s \sum_n w_n^{\sigma,s}(x)\, \Theta_n^{\sigma,s}(\theta)\, e^{is\phi}. \tag{39}$$

Using this expression along with the appropriate expansions for v_0^{σ} and u_0^{σ} and substituting into the first order lower boundary condition (15), it can be seen that the only non-zero terms in the sum over s in (39) correspond to $s = s_0 \pm m$. Making use of the orthogonality properties of the Hough functions, the boundary condition becomes

$$w_n^{\sigma,s_0\pm m}(0) = \frac{H}{a} \sum_{n'} u_n^{\sigma;s_0}(0) \left\{ i \int_0^{\pi} a_{\pm m}(\theta)\, V_n^{\sigma;s_0}(\theta)\, \Theta_n^{\sigma,s_0\pm m}(\theta)\, d(\cos\theta) \right. \tag{40}$$

$$\left. + \int_0^{\pi} b_{\pm m}(\theta)\, U_n^{\sigma;s_0}(\theta)\, \Theta_n^{\sigma,s_0\pm m}(\theta)\, d(\cos\theta) \right\}.$$

In obtaining this expression, use has been made of (30). The right hand side of (40) can be expressed directly in terms of the vertical mean zero order tidal temperature field using (34);

$$w_n^{\sigma,s_0\pm m}(0) = -\frac{1}{2}\,\frac{i\sigma RH}{4a^2\Omega^2}\,e^{\pm i\delta_m}\sum_{n'} N_{n,n'}^{s_0,\pm m}\,\frac{H/h_{n'}^{\sigma,s_0}}{H/h_{n'}^{\sigma,s_0}-1}\left\langle \delta T_{n'}^{\sigma,s_0}\right\rangle \tag{41}$$

where

$$\begin{aligned} N_{n,n'}^{s_0,\pm m} &= \int_0^{\pi}\frac{\partial}{\partial\theta}\left[\frac{\xi_m(\theta)}{H}\right] U_{n'}^{\sigma,s_0}(\theta)\,\Theta_n^{\sigma,s_0\pm m}(\theta)\,d(\cos\theta) \\ &\mp m\int_0^{\pi}\frac{1}{\sin\theta}\,\frac{\xi_m(\theta)}{H}\,V_{n'}^{\sigma,s_0}(\theta)\,\Theta_n^{\sigma,s_0\pm m}(\theta)\,d(\cos\theta). \end{aligned} \tag{42}$$

Explicit solutions of the vertical structure equation (38) with the inhomogeneous lower boundary condition (41) must now be considered. With the definition

$$\beta_n^{\sigma,s} = \begin{cases} \sqrt{\left|\kappa\,\dfrac{H}{h_n^{\sigma,s}}-\dfrac{1}{4}\right|}\,; & \kappa\,\dfrac{H}{h_n^{\sigma,s}}-\dfrac{1}{4}>0 \\ i\sqrt{\left|\kappa\,\dfrac{H}{h_n^{\sigma,s}}-\dfrac{1}{4}\right|}\,; & \kappa\,\dfrac{H}{h_n^{\sigma,s}}-\dfrac{1}{4}<0 \end{cases} \tag{43}$$

the general solution can be written

$$y_n^{\sigma,s} = A_n^{\sigma,s}e^{i\beta_n^{\sigma,s}x} + B_n^{\sigma,s}e^{-i\beta_n^{\sigma,s}x} \tag{44}$$

where $A_n^{\sigma,s}$ and $B_n^{\sigma,s}$ are arbitrary constants. For the case when κ H/h - 1/4 > 0 (vertically propagating solutions), it will be assumed that no downward propagation of energy occurs as $x \to \infty$ with the result that $B_n^{\sigma,s} = 0$. When κ H/h - 1/4 < 0 (vertically evanescent solutions), the requirement that the kinetic energy density remain bounded as $x \to \infty$ again leads to $B_n^{\sigma,s} = 0$. $A_n^{\sigma,s}$ can be evaluated by substitution into (41), using (31) to express the vertical velocity in terms of $y_n^{\sigma,s}$. The result is

$$A_n^{\sigma,s_0\pm m} = -\frac{1}{2}\,\frac{i\sigma R}{4\gamma a^2\Omega^2}\,\frac{H}{h_n^{\sigma,s_0\pm m}}\left(i\beta_n^{\sigma,s_0\pm m} + \frac{H}{h_n^{\sigma,s_0\pm m}} - \frac{1}{2}\right)^{-1} e^{\pm i\delta_m}$$

$$\cdot \sum_{n'} N_{n,n'}^{s_0,\pm m}\,\frac{H/h_{n'}^{\sigma,s_0}}{H/h_{n'}^{\sigma,s_0} - 1}\left\langle \delta T_{n'}^{\sigma,s_0}\right\rangle . \tag{45}$$

From (28), the height dependent coefficients for the first order tidal temperature field can be written

$$\delta T_n^{\sigma,s_0\pm m}(x) = -\frac{\kappa\gamma gH}{i\sigma R} A_n^{\sigma,s_0\pm m}\, e^{(1/2 + i\beta_n^{\sigma,s_0\pm m})x} . \tag{46}$$

Finally, the total first order tidal temperature field produced by the interaction of the zero order tidal wave of wavenumber s_0 with topography of wavenumber m is

$$\delta T_1(\theta, \phi, x, t) = \left[\sum_n \delta T_n^{\sigma, s_0+m}(x)\, \Theta_n^{\sigma, s_0+m}(\theta)\right] e^{i[(s_0+m)\phi+\sigma t]}$$

$$+ \left[\sum_n \delta T_n^{\sigma, s_0-m}(x)\, \Theta_n^{\sigma, s_0-m}(\theta)\right] e^{i[(s_0-m)\phi+\sigma t]}. \tag{47}$$

The first order tidal surface pressure and velocity fields can be written

$$\delta p_1(\theta, \phi, 0, t) = \left[\sum_n \delta p_n^{\sigma, s_0+m}(0)\, \Theta_n^{\sigma, s_0+m}(\theta)\right] e^{i[(s_0+m)\phi+\sigma t]}$$

$$+ \left[\sum_n \delta p_n^{\sigma, s_0-m}(0)\, \Theta_n^{\sigma, s_0-m}(\theta)\right] e^{i[(s_0-m)\phi+\sigma t]}, \tag{48}$$

$$u_1(\theta, \phi, x, t) = \left[\sum_n u_n^{\sigma, s_0+m}(x)\, U_n^{\sigma, s_0+m}(\theta)\right] e^{i[(s_0+m)\phi+\sigma t]}$$

$$+ \left[\sum_n u_n^{\sigma, s_0-m}(x)\, U_n^{\sigma, s_0-m}(\theta)\right] e^{i[(s_0-m)\phi+\sigma t]}, \tag{49}$$

$$v_1(\theta, \phi, x, t) = \left[\sum_n v_n^{\sigma, s_0+m}(x)\, V_n^{\sigma, s_0+m}(\theta)\right] e^{i[(s_0+m)\phi+\sigma t]}$$

$$+ \left[\sum_n v_n^{\sigma, s_0-m}(x)\, V_n^{\sigma, s_0-m}(\theta)\right] e^{i[(s_0-m)\phi+\sigma t]}, \tag{50}$$

where

$$\delta p_n^{\sigma, s_0 \pm m}(0) = p_0(0) \frac{\gamma}{i\sigma} \frac{h_n^{\sigma, s_0 \pm m}}{H} \left(i\beta_n^{\sigma, s_0 \pm m} - \frac{1}{2} \right) A_n^{\sigma, s_0 \pm m} \tag{51}$$

$$u_n^{\sigma, s_0 \pm m}(x) = \frac{\gamma g h_n^{\sigma, s_0 \pm m}}{4a\Omega^2} \left(i\beta_n^{\sigma, s_0 \pm m} - \frac{1}{2} \right) A_n^{\sigma, s_0 \pm m} e^{(1/2 + i\beta_n^{\sigma, s_0 \pm m})x} \tag{52}$$

$$v_n^{\sigma, s_0 \pm m}(x) = i u_n^{\sigma, s_0 \pm m}(x). \tag{53}$$

From (47)-(50) it can be seen that the first order effect of the presence of large scale topography is to excite waves with longitudinal wavenumbers equal to both the sum and the difference of the zero order wavenumber and the topography wavenumber. The phase speeds of these waves will in general be different from the speed of the solar excitation. Note that for $m > s_0$, eastward propagating as well as westward propagating waves can occur.

The interaction of the tidal regime with large scale planetary topography has been studied here by considering the kinematic effects of the lower boundary. The calculations have been carried through first order in the ratio of the surface elevation to the atmospheric scale height. For Mars, this ratio, while less than unity on a planetary scale, is not particularly small. However, the model should serve as a useful tool for achieving an understanding of the observational data.

Comparison of Theoretical and Observational Results

The theoretical derivations of the preceeding section will now be applied to the Mariner 9 observations. The zero order diurnal temperature amplitude and phase is approximated by a model derived from the Mariner 9 IRIS data by Pirraglia and Conrath (1974). Its representation in terms of Hough functions is shown in Figure 4; the individual Hough amplitudes and phases are listed in Table 1. The phase has been chosen such that $\pi/2$ corresponds to a diurnal wave maximum at 18 hours local time. The Hough function notation corresponds to that employed by Chapman and Lindzen (1970). Negative subscripts denote modes corresponding to negative equivalent depths.

The large scale topography is approximated by the truncated expansion

$$\xi/H = \sum_{m=1}^{3} \sum_{\ell=m}^{3} (C_\ell^m \cos m\phi + S_\ell^m \sin m\phi) P_\ell^m(\theta) \qquad (54)$$

where $P_\ell^m(\theta)$ is the (unnormalized) associated Legendre function as defined by Jahnke and Emde (1945). Longitudinally symmetric (m = 0) components of topography can modify the migrating diurnal tidal wave, but cannot excite new tidal modes through first order interaction. The effects of the m = 0 components cannot be removed from the zonally averaged data on which the model of Table 1 and Figure 4 is based. Thus the "zero order" temperature field used in the calculations already includes the contributions from the zonally symmetric topography, so these terms have been omitted from equation (54). The coefficients used in the expansion were taken from preliminary harmonic fits to the

geoid and topography (E. J. Christensen, private communication, 1974) and are given in Table 2.

The first order perturbation tidal fields were calculated for each of the six components of topography contained in (54). In each case the eight lowest order Hough functions were retained in the expansion in (45). The total first order temperature perturbation was calculated by summing the contributions from all topography components. The results for the 2mb level are shown as solid curves in Figures 1, 2, and 3. A surface pressure of 5mb and a scale height of 11km were assumed. As plotted in the figures, the first order perturbations are combined with the zero order diurnal wave so a direct comparison with the observational data points can be made. The amplitude and shape of the calculated perturbations appear to be in reasonable agreement with the observations.

While a total of forty-eight Hough modes are included in the calculations shown, only a few make significant contributions. Those modes with amplitudes at 2mb in excess of 1°K are listed in Table 3. The $\Theta_1^{1,-1}$ contribution which dominates the solution, is a wave number one mode with a phase velocity equal in magnitude but opposite in direction to the solar excitation. This mode corresponds to a positive equivalent depth, but with $h > 4\kappa H$, and is therefore vertically evanescent. The phases of the tidal fields associated with this type of mode are independent of height while the amplitude grows exponentially.

Examination of temperature data up to the upper limit of the IRIS sounding range at ~ 0.1 mb tends to confirm this behavior. However, at the upper levels the calculated temperature perturbation amplitude tends to exceed that indicated by the data. This is possibly due to the omission of dissipative effects from the theoretical model which would tend to limit the amplitude at high levels. The remaining three modes listed in Table 3 are also eastward traveling waves, and since their equivalent depths satisfy the condition $0 < h < 4\kappa H$ they are vertically propagating. The contributions of these waves to the total first order perturbation fields in the lower atmosphere are small compared to the $\Theta_1^{1,-1}$ mode. However, they are of some interest because they are potentially capable of transporting energy from the lower to the upper atmosphere.

The strong excitation of the $\Theta_1^{1,-1}$ mode is related to the fact that the equivalent depth of this mode is of the same order of magnitude as the atmospheric scale height. Examination of (45) along with (43) indicates that in the absence of dissipation, resonance can occur when $H = (1-\kappa)\, h$. For $\kappa = 0.23$, the resonant scale height would be 9.44 km corresponding to a mean basic state temperature of 185°K. In the present model, the value H = 11 km (corresponding to a basic state temperature of 215°K) is sufficiently far from the actual resonance point that the neglect of dissipative effects probably does not introduce serious error in the calculation of the coefficient A in equation (45). For example an estimate assuming linear radiative damping indicates that A changes by less than 10 per cent for a damping time of 1 day.

Examination of the matrix elements $N_{nn'}$, which provide measures of the relative efficiency of the various zero order perturbation modes for exciting 1st order modes, indicates that the interaction of the $\Theta_1^{1,1}$ zero order mode with the P_2^2 component of topography is primarily responsible for exciting the $\Theta_1^{1,-1}$ mode. P_2^2 represents the lowest order component of topography with longitudinal wave number 2 and is symmetric with respect to the equator. $\Theta_1^{1,1}$ is the lowest order diurnal tidal mode with positive equivalent depth and is also symmetric with respect to the equator. The strong excitation of the $\Theta_1^{1,-1}$ mode by the wavenumber 2 topography on Mars was previously predicted by Zurek (1976).

Having identified the P_2^2 component of topography as the principle source of excitation, is now possible to investigate the effects of this excitation on the atmospheric dynamics during the dust storm conditions. The amplitudes and phases of the near-surface tidal wind components resulting from the P_2^2 topography term, as calculated from (49), (50), (52), and (53), are shown in Figures 5 and 6. The zonal wind component of this eastward traveling 1st order wave is dominant at low latitudes, reaching a maximum amplitude of about 16m sec^{-1} at the equator. Near-surface wind amplitudes and phases of the zero order diurnal tidal wave, based on the model of Pirraglia and Conrath (1974), are also shown in the figures. The combination of the westward traveling zero order wave with the eastward traveling first order wave results in a diurnally fluctuating wind field, the amplitude of which is dependent on longitude as well as

latitude. This dependence is displayed in Figures 7 and 8. The presence of the first order wave enhances the diurnal amplitude in some locations while diminishing it in others. Of particular interest is the increase in zonal wind to amplitudes greater than 40m sec^{-1} over relatively small areas near -30° latitude. The tidal winds will be augmented by the presence of a zonally symmetric wind component (Pirraglia 1975) and possibly by topographic effects on a local scale. This suggests that the free stream threshold velocity for the injection of dust into the atmosphere may have been exceeded in these regions during some time period each day throughout the course of the storm.

Returning now to the three vertically propagating waves listed in Table 3, it is of interest to calculate the associated vertical energy flux. The time averaged flux associated with each mode can be written (Siebert, 1961)

$$W_n(\theta) = \frac{\gamma^2 h_n P_0(0)}{2\sigma} \operatorname{Im}\left(y_n^* \frac{dy_n}{dx}\right)[\Theta_n(\theta)]^2. \qquad (55)$$

The combined energy flux of the three vertically propagating modes is shown as a function of latitude in Figure 9. For comparison, the vertical energy flux in the earth's atmosphere due to the diurnal tide is estimated by Lindzen (1967) to be ~ 7 ergs sec^{-1} cm^{-2} at the equator. The flux shown in Figure 9 represents the energy propagating upward from the surface which serves as a source of excitation for these modes. The extent to which the energy actually propagates into the upper atmosphere is an open question at this point. To study this aspect

further would require a more detailed modeling of the higher levels. However, the calculations presented here indicated that topographically excited vertically propagating modes do represent a potential source of energy for the upper atmosphere during dust storm conditions.

Summary and Conclusions

The Mariner 9 IRIS data during the 1971 dust storm show well defined topography-correlated temperature perturbations superposed on the strong diurnal thermal tide. These perturbations appear to result from the topographic excitation of additional tidal modes which do not follow the sun. Using a first order perturbation calculation, it was found that the topography component of longitudinal wave number 2 provides a strong source of excitation. In particular, the $\Theta_1^{1,-1}$ mode was found to be dominant. This is an eastward traveling wave-number one mode with an equivalent depth comparable to the atmospheric scale height. The good quantitative agreement between the theoretically calculated and observed temperature perturbations indicates that the principal tidal modes have been properly identified. The results presented here support the conclusion of Zurek (1976) that the $\Theta_1^{1,-1}$ mode should be strongly excited.

Estimates of the near surface tidal wind fields indicate strong contributions from topographically excited modes at low latitudes. Near 30° south where maximum winds are found, the amplitude of the diurnally fluctuating zonal wind is found to be increased to over 40 m sec^{-1} in limited areas. Although the

quantitative results obtained here must be regarded with due caution because of the crudeness of the model, they do indicate that the presence of large scale topography may enhance winds sufficiently at some locations to contribute to the injection of dust into the atmosphere during dust storm conditions.

The calculations indicate that vertically propagating modes are also excited by topography. While these modes produce little significant effect on the temperature and wind fields of the lower atmosphere, they do result in a strong energy flux upward from the surface. These modes thus represent a possible source of energy for the upper atmosphere during a storm. However, to estimate the extent to which this energy actually propagates to the upper levels requires a more detailed modeling of the atmosphere than has been considered here.

Acknowledgements

The extensive computer programming required for the numerical calculations was carried out by H. W. Sagges. M. F. Flasar, R. A. Hanel, and J. A. Pirraglia provided valuable comments on the manuscript. Assistance from V. G. Kunde and J. C. Pearl in many areas of this work is appreciated.

APPENDIX

The vertical structure equation for an isothermal atmosphere (19) and the expression for the corresponding tidal temperature field (28) can be combined to eliminate J yielding

$$\frac{d^2y}{dx^2} - \frac{1}{4}\, y = \frac{i\sigma R}{\gamma g h}\, \delta T e^{-x/2} \qquad \text{(A-1)}$$

where all subscripts and superscripts designating modes have been surpressed. This can be regarded as a vertical structure equation with $\delta T(x)$ as the driving term. An expression for $\langle \delta T \rangle$, the density weighted average of δT, can be obtained by multiplying both sides of (A-1) by $e^{-x/2}$ and integrating to obtain

$$\frac{i\sigma R}{\gamma g h} \langle \delta T \rangle = \int_0^\infty e^{-x/2} \frac{d^2y}{dx^2}\, dx - \frac{1}{4} \int_0^\infty e^{-x/2}\, y\, dx. \qquad \text{(A-2)}$$

Integrating the first term on the right hand side by parts twice and assuming

$$\left(\frac{dy}{dx} + \frac{1}{2}\, y\right) e^{-x/2} \xrightarrow[x \to \infty]{} 0$$

gives

$$\frac{i\sigma R}{\gamma g h} \langle \delta T \rangle = -\left(\frac{dy}{dx}\right)_{x=0} - \frac{1}{2}\, y(0). \qquad \text{(A-3)}$$

The zero order lower boundary condition (32) can be employed to eliminate $(dy/dx)_{x=0}$ resulting in

$$\frac{i\sigma R}{\gamma g h} \langle \delta T \rangle = \left(\frac{H}{h} - 1 \right) \; y(0). \qquad \text{(A-4)}$$

This provides the desired expression for y(0).

REFERENCES

Cain, D. L., A. J. Kliore, B. L. Seidel, and M. J. Sykes, 1972: The shape of Mars from the Mariner 9 occultations. Icarus, 17, 517-524.

Chapman, S., and R. S. Lindzen, 1970: Atmospheric Tides. Dordrecht, Holland, Reidel Publishing Co., 200 pp.

Conrath, B. J., and I. Revah, 1972: A review of nonstatistical techniques for the estimation of vertical atmospheric structure from remote infrared measurements. In "Proceedings of a Workshop on the Mathematics of Profile Inversion" (L. Colin, Ed.), NASA, TMX-62150.

Conrath, B., R. Curran, R. Hanel, V. Kunde, W. Maguire, J. Pearl, J. Pirraglia, and J. Welker, 1973: Atmospheric and surface properties of Mars obtained by infrared spectroscopy on Mariner 9. J. Geophys. Res., 78, 4267-4278.

Downs, G. S., P. E. Reichley, and R. R. Green, 1975: Radar measurements of Martian topography and surface properties: the 1971 and 1973 oppositions. Icarus, 26, 273-312.

Hanel, R., B. Conrath, W. Hovis, V. Kunde, P. Lowman, W. Maguire, J. Pearl, J. Pirraglia, C. Prabhakara, and B. Schlachman, 1972: Investigation of the Martian environment by infrared spectroscopy on Mariner 9. Icarus, 17, 423-442.

Hord, C. W., K. E. Simmons, and L. K. McLaughlin, 1974: Mariner 9 ultraviolet spectroscopy experiment: pressure-altitude measurements on Mars. Icarus, 21, 292-302.

Jahnke, E., and F. Emde, 1945: Tables of Functions with Formulae and Curves. New York, Dover Publications, 306pp.

Kliore, A. J., D. L. Cain, G. Fjeldbo, B. L. Seidel, M. J. Sykes, and S. I. Rasool, 1972: The atmosphere of Mars from Mariner 9 radio occultation measurements. Icarus, 17, 484-516.

Leovy, C. B., G. A. Briggs, A. T., Young, B. A. Smith, J. B. Pollack, E. N. Shipley, and R. L. Wildey, 1972: The Martian atmosphere: Mariner 9 television experiment progress report. Icarus, 17, 373-393.

Leovy, C. B., R. W. Zurek, and J. B. Pollack, 1973: Mechanisms for Mars dust storms. J. Atmos. Sci., 30, 749-762.

Lindzen, R. S., 1967: Thermally driven diurnal tide in the atmosphere. Q. J. Roy. Met. Soc., 93, 18-42.

Lindzen, R. S., 1970: The application and applicability of terrestrial atmospheric tidal theory to Venus and Mars. J. Atmos. Sci., 27, 536-549.

Pirraglia, J. A. 1975: Polar symmetric flow of a viscous compressible atmosphere: an application to Mars. J. Atmos. Sci., 32, 60-72.

Pirraglia, J. A., and B. J. Conrath, 1974: Martian tidal pressure and wind fields obtained from the Mariner 9 infrared spectroscopy experiment. J. Atmos. Sci., 31, 318-329.

Siebert, M., 1961: Atmospheric tides. Adv. in Geophys., 7, 105-187.

Zurek, R. W., 1976: Diurnal tide in the Martian atmosphere. J. Atmos. Sci., 33, 321-337.

TABLE 1

Temperature amplitudes and phases for the Hough function representation of the zero order depth averaged diurnal thermal tide.

Hough Mode	Equivalent Depth (KM)	Amplitude (K)	Phase
$\Theta_1^{1,1}$	.49	3.60	$-\pi/2$
$\Theta_3^{1,1}$	.085	.94	$\pi/2$
$\Theta_{-1}^{1,1}$	1044.2	4.40	$\pi/2$
$\Theta_{-2}^{1,1}$	-8.66	11.44	$\pi/2$
$\Theta_{-4}^{1,1}$	-5.02	3.46	$-\pi/2$

TABLE 2

Coefficients for spherical harmonic representation of the ratio of the surface elevation to the atmospheric scale height ξ/H.

m	ℓ	C_ℓ^m	S_ℓ^m
1	1	.00326	-.13786
1	2	.04050	-.00620
1	3	-.00242	-.04287
2	2	-.06410	.04943
2	3	-.01072	.01249
3	3	.00545	.00910

TABLE 3

The Hough modes most highly excited by topography. The topography mode responsible for the excitation is given in the final column.

Hough Mode	Temperature Amplitude at 2mb (K)	Phase (Radians)	Equivalent Depth (KM)	Vertical Wave Length (Scale Heights)	Topography Mode
$\Theta_1^{1,-1}$	7.09	-2.23	12.3	3.45*	P_2^2
$\Theta_3^{1,-1}$	1.11	-2.89	0.369	2.44	P_2^2
$\Theta_2^{1,-2}$	2.01	3.04	3.45	8.98	P_3^3
$\Theta_4^{1,-2}$	1.30	-0.87	0.295	2.18	P_3^3

*Vertically evanescent. The value given is the vertical distance over which the amplitude changes by a factor of e.

FIGURE CAPTIONS

Figure 1 – Comparison of atmospheric temperatures at the 2mb level with topographic relief. The temperature data points represent individual measurements obtained within the latitude interval -20° to -30° for the local time intervals indicated. The solid lines represent the results of model calculations for -25° latitude and 6.5 and 17.5 hours local time. The mean surface elevation expressed in units of atmospheric scale height for the latitude interval 0° to -45° is shown in the lower panel.

Figure 2 – Similar to Figure 1 except for the latitude interval -30° to -40°.

Figure 3 – Similar to Figure 1 except for the latitude interval -40° to -50°.

Figure 4 – Amplitude and phase of depth averaged temperature employed as a zero order model. A phase of $\pi/2$ corresponds to a maximum at 18 hours local time.

Figure 5 – Amplitudes and phases of the zero and first order contributions to the meridional component of the diurnal wind field. The zero order contribution is a westward traveling wave while the first order contribution is an eastward traveling wave.

Figure 6 – Same as Figure 5 except for the zonal component of the diurnal wind.

Figure 7 – Diurnal amplitude of meridional wind as a function of latitude and longitude. The amplitude shown results from a combination of the zero order and first order waves. The wind speeds shown are in m sec^{-1}.

Figure 8 – Same as Figure 7 except for zonal wind.

Figure 9 – Vertical energy flux due to topographically excited vertically propagating tidal modes.

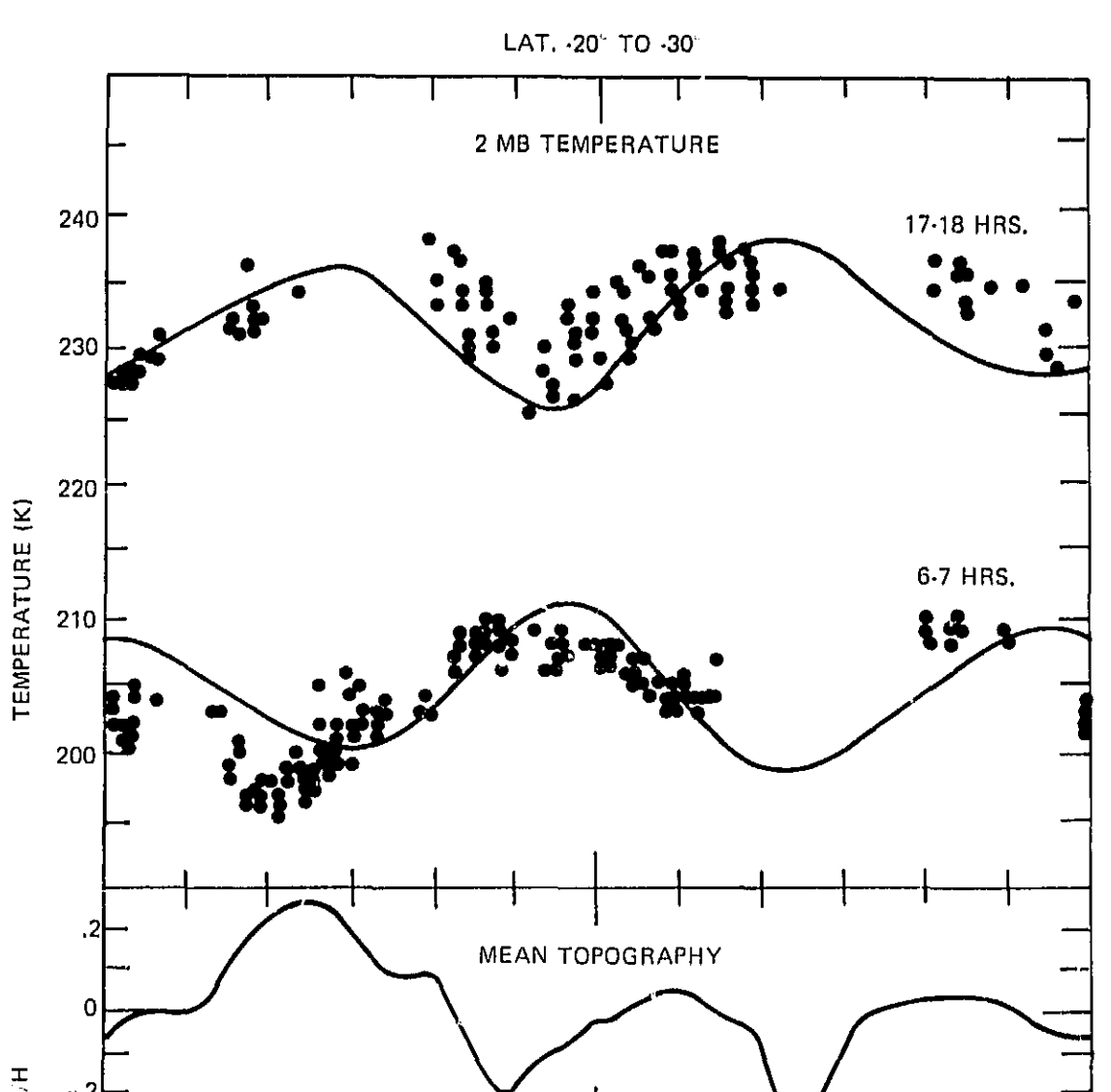

Figure 1. Comparison of atmospheric temperatures at the 2mb level with topographic relief. The temperature data points represent individual measurements obtained within the latitude interval -20° to -30° for the local time intervals indicated. The solid lines represent the results of model calculations for -25° latitude and 6.5 and 17.5 hours local time. The mean surface elevation expressed in units of atmospheric scale hieght for the latitude interval 0° to -45° is shown in the lower panel.

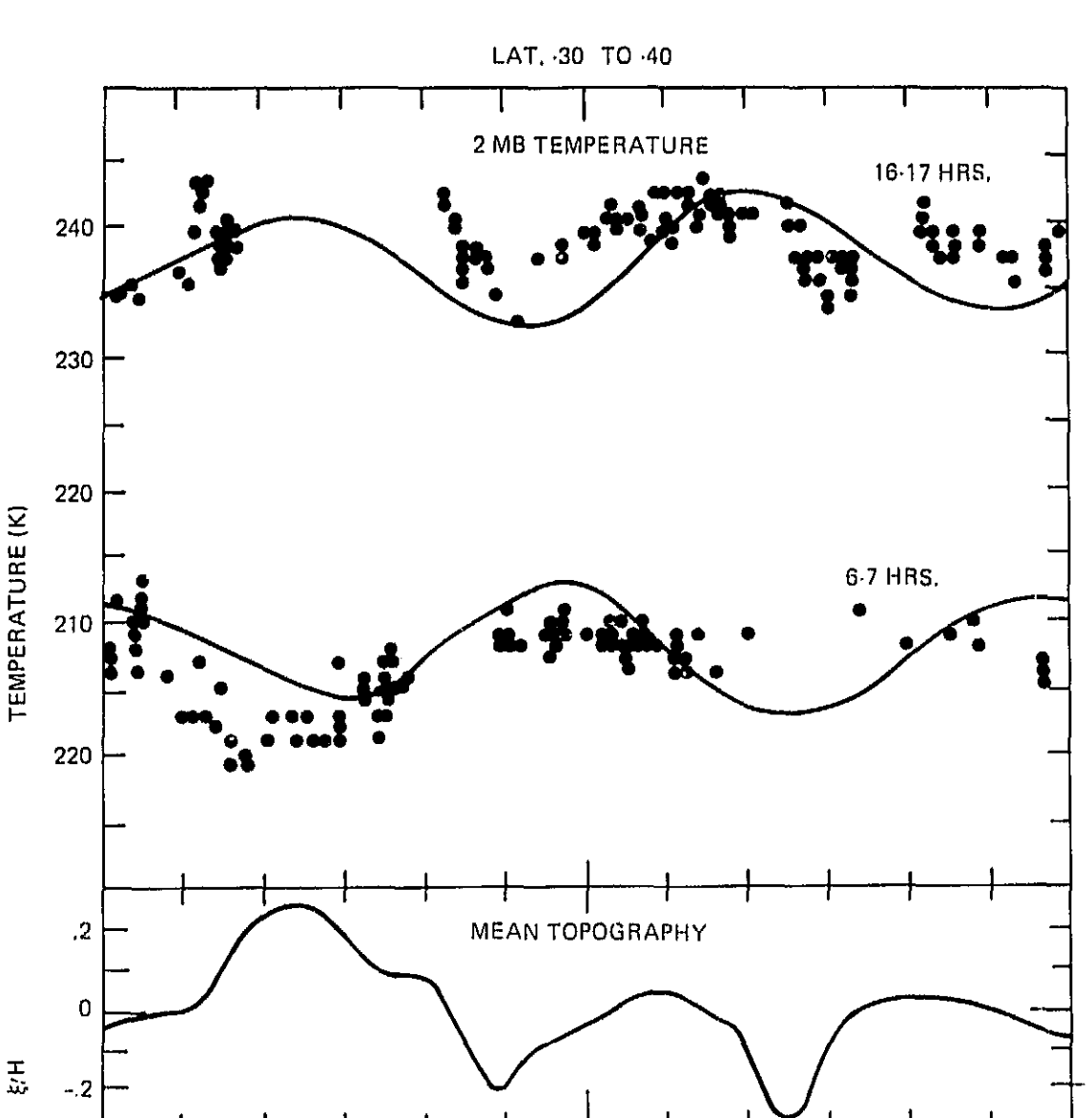

Figure 2. Similar to Figure 1 except for the latitude interval -30° to -40°.

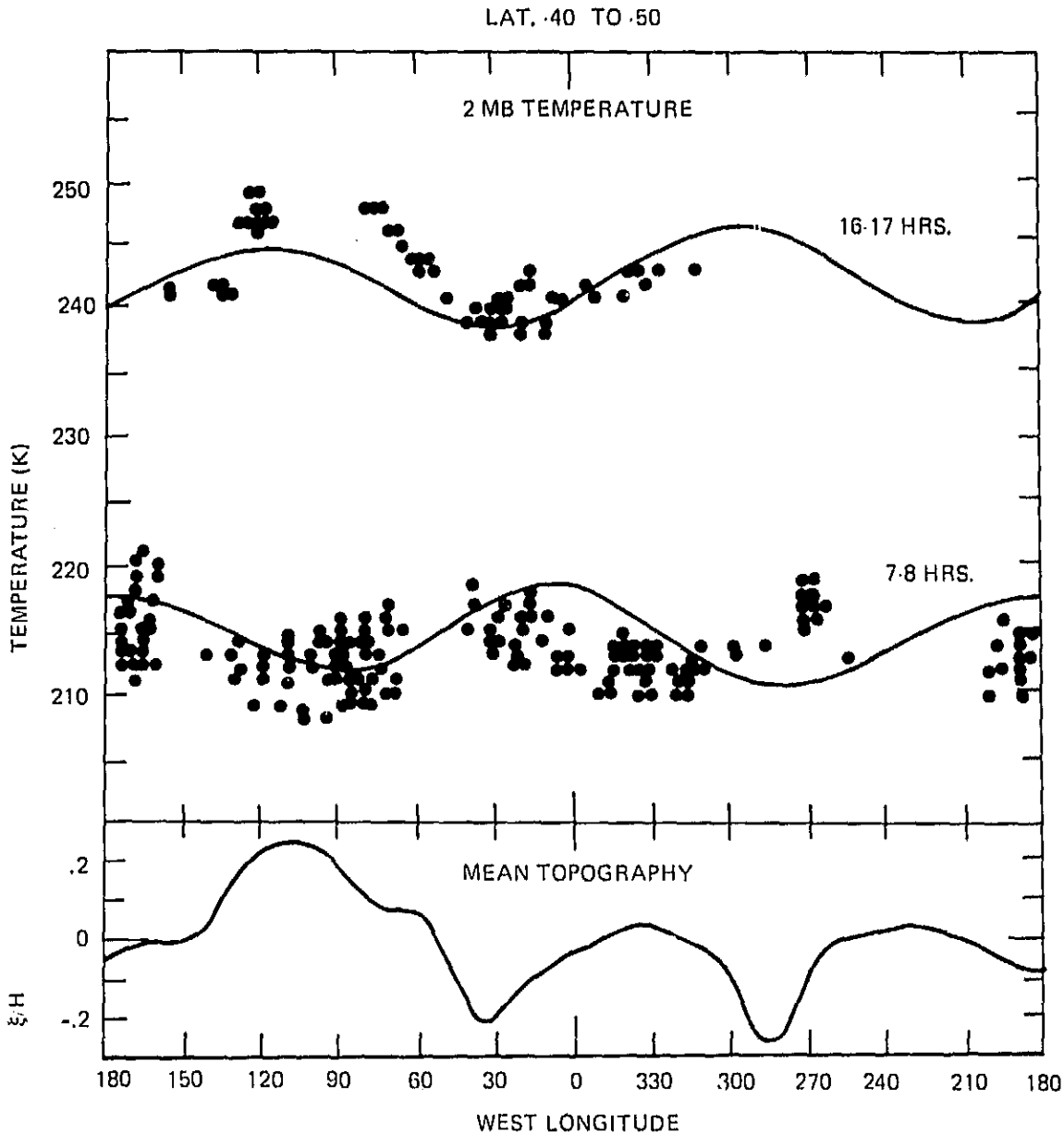

Figure 3. Similar to Figure 1 except for the latitude interval -40° to -50°.

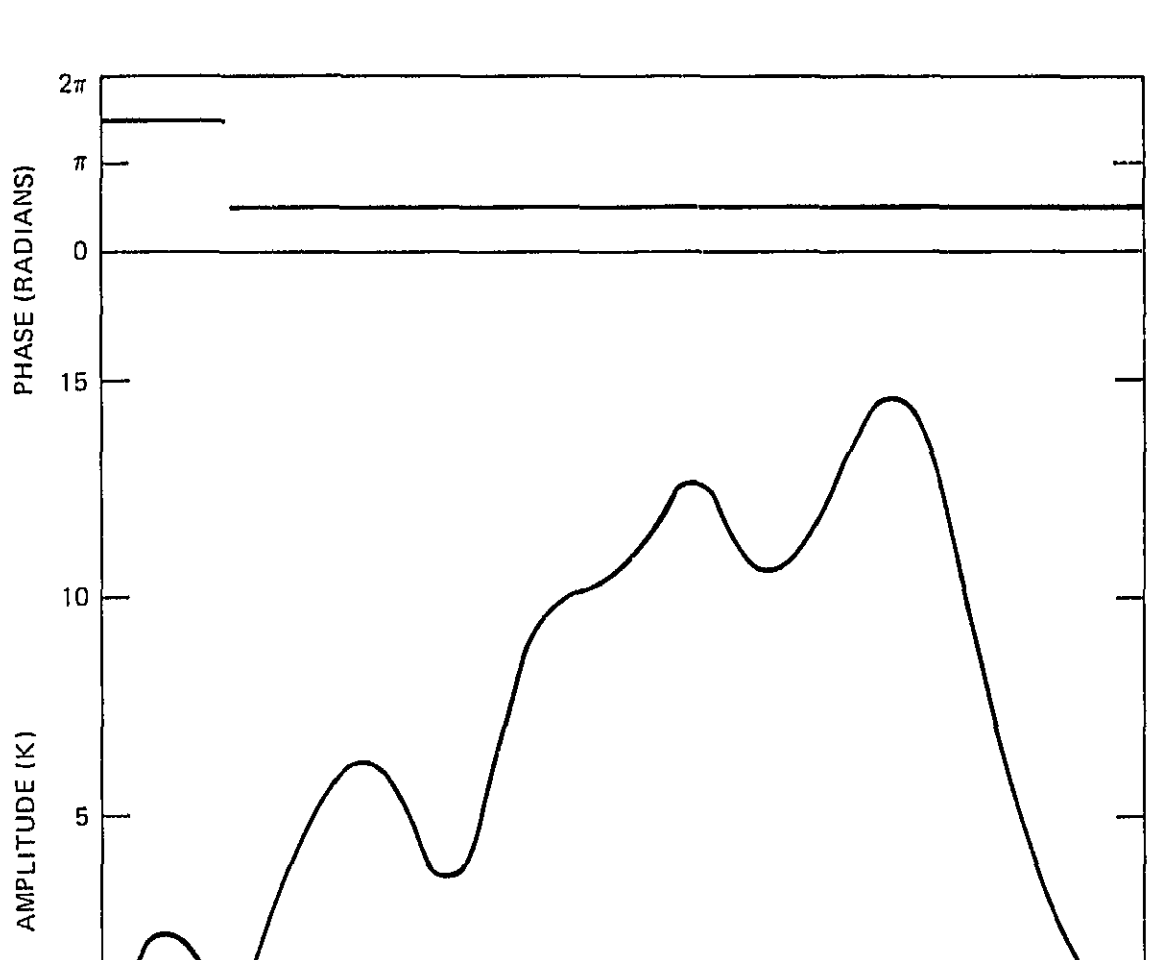

Figure 4. Amplitude and phase of depth averaged temperature employed as a zero order model. A phase of $\pi/2$ corresponds to a maximum at 18 hours local time.

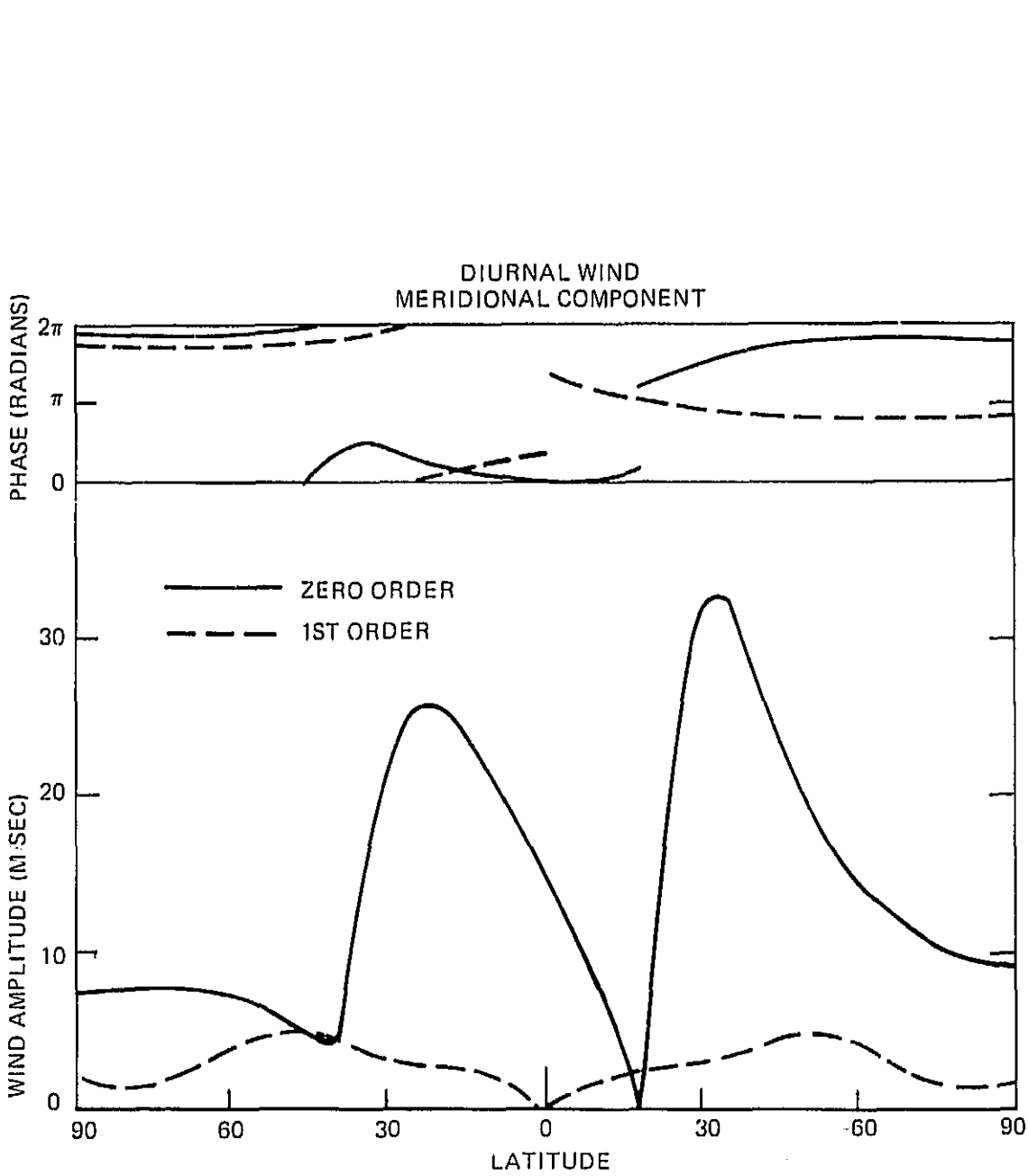

Figure 5. Amplitudes and phases of the zero and first order contributions to the meridional component of the diurnal wind field. The zero order contribution is a westward traveling wave while the first order contribution is an eastward traveling wave.

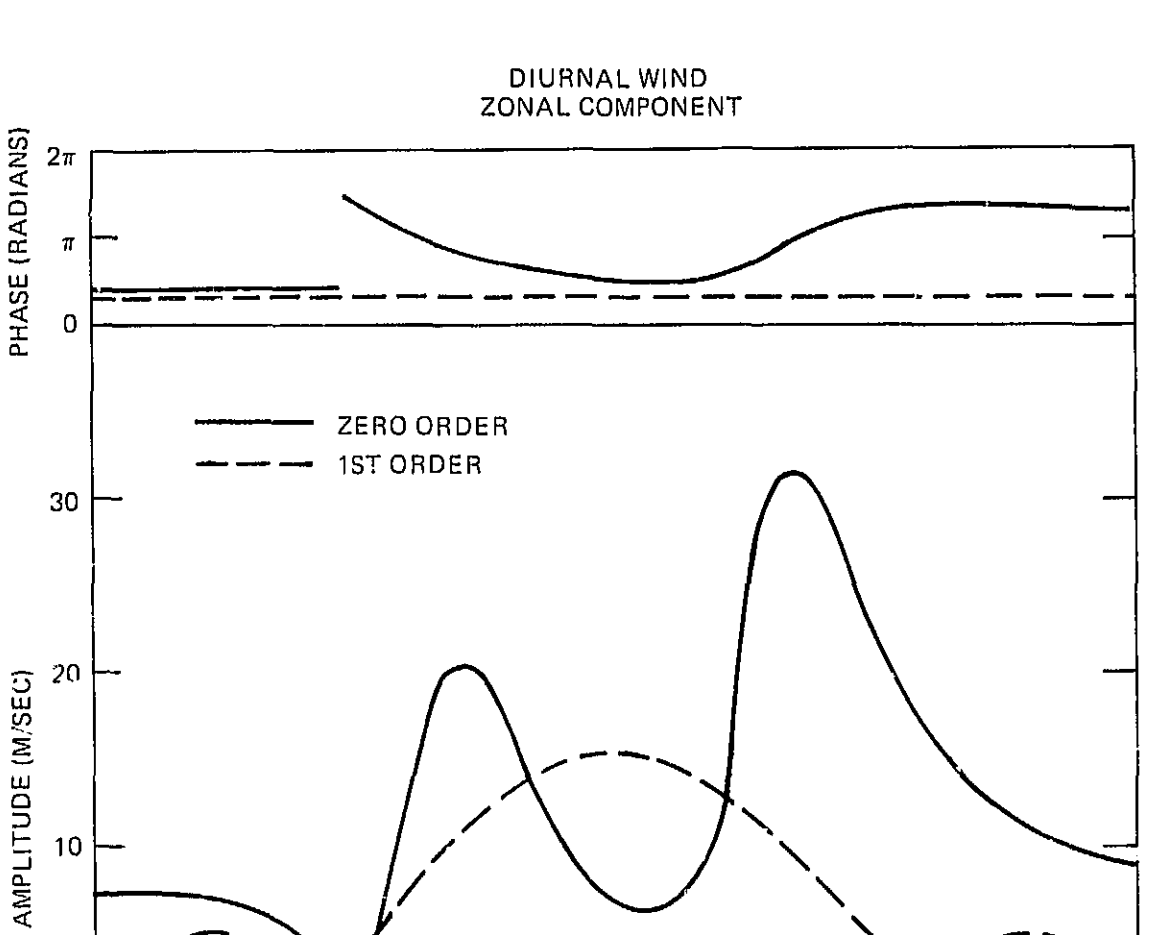

Figure 6. Same as Figure 5 except for the zonal component of the diurnal wind.

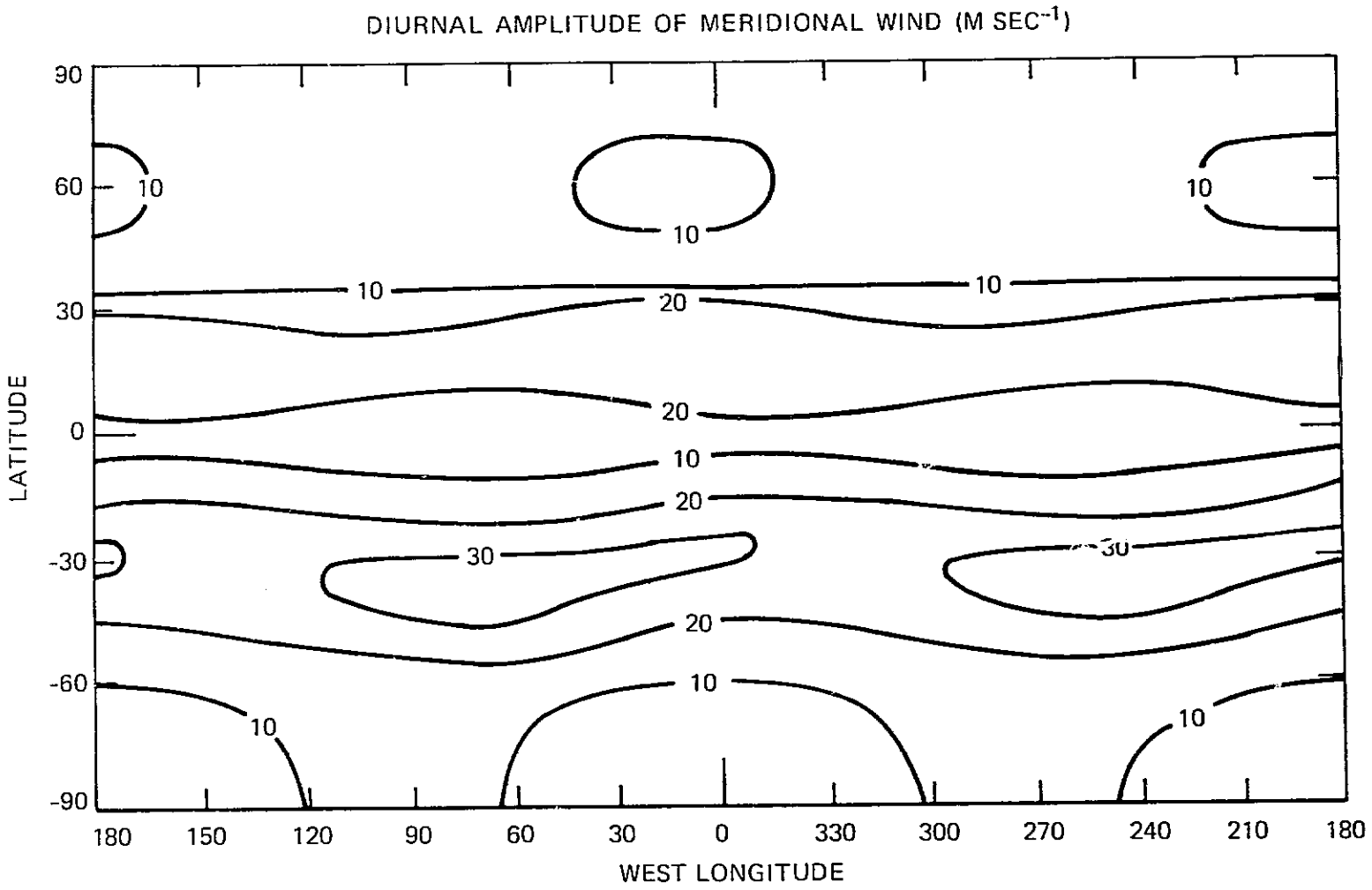

Figure 7. Diurnal amplitude of meridional wind as a function of latitude and longitude. The amplitude shown results from a combination of the zero order and first order waves. The wind speeds shown are in m sec^{-1} .

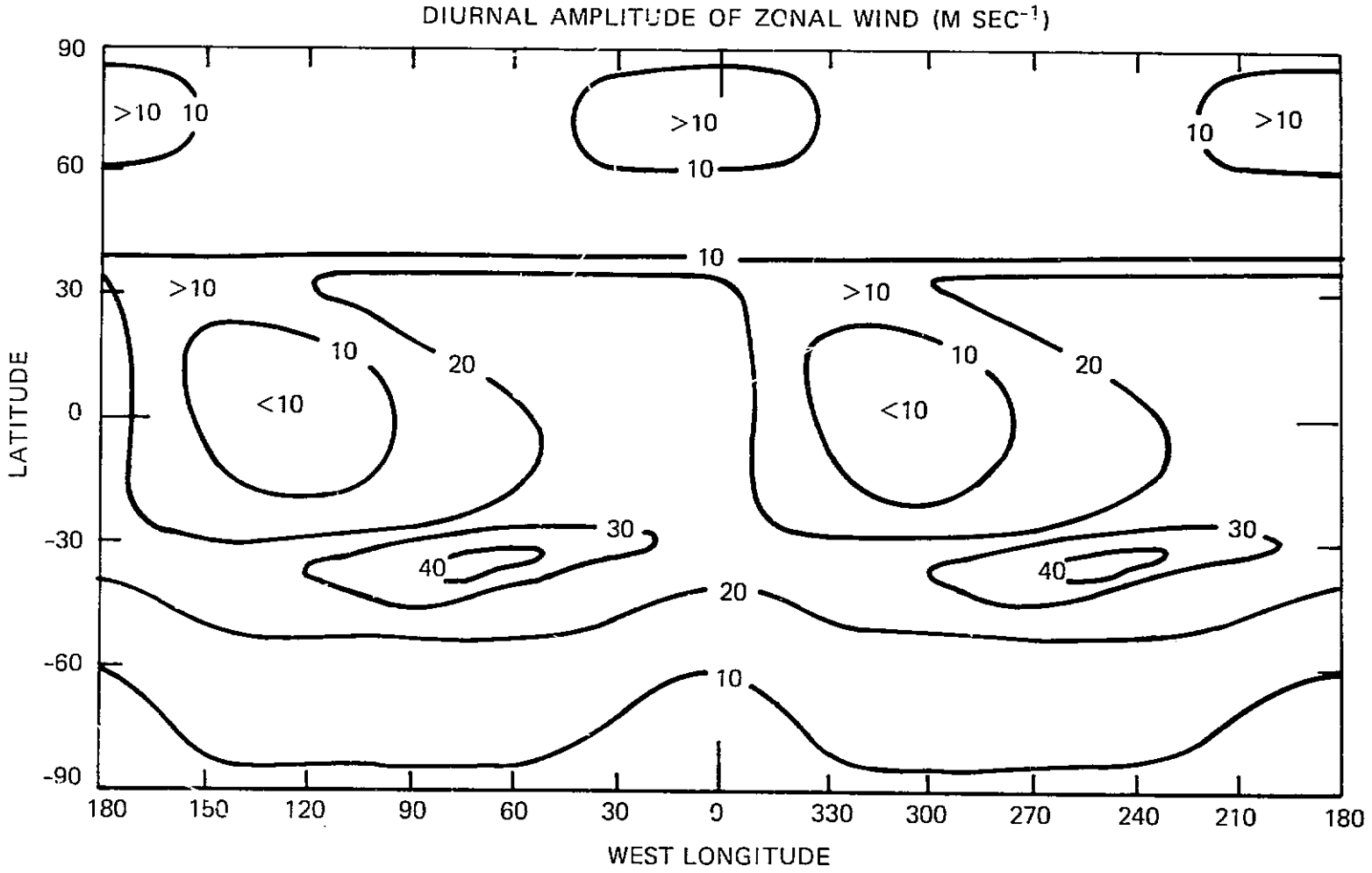

Figure 8. Same as Figure 7 except for zonal wind.

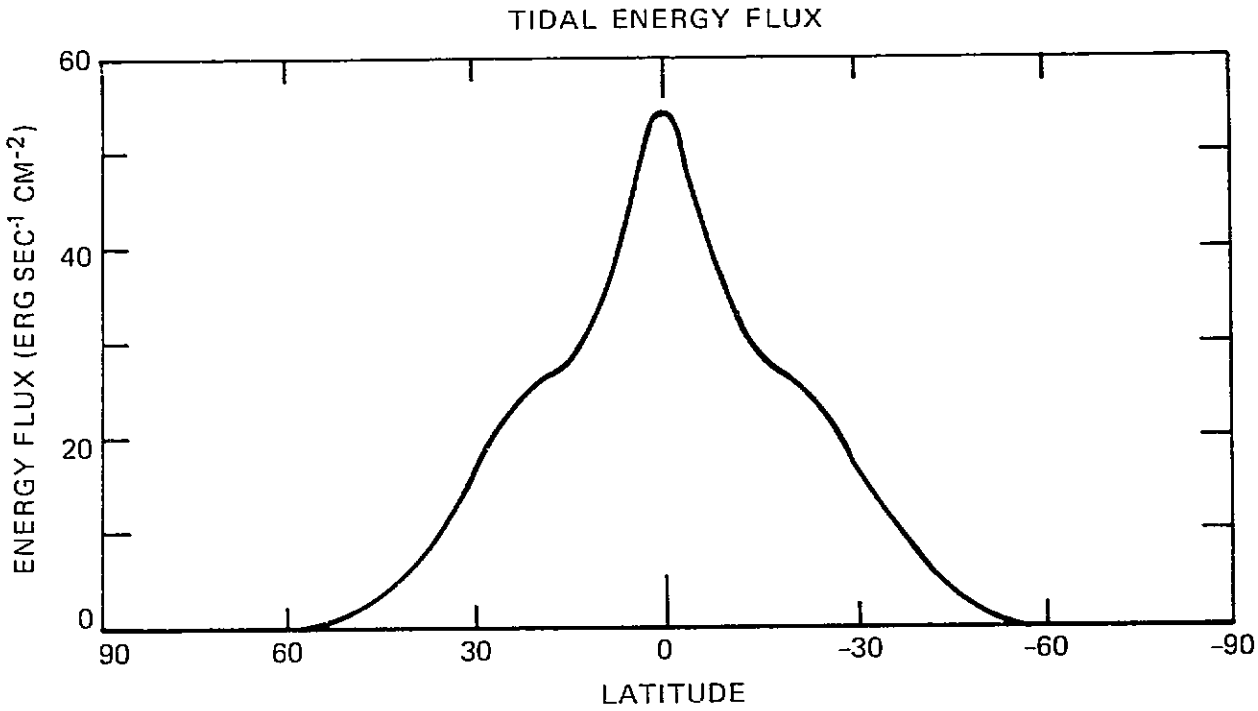

Figure 9. Vertical energy flux due to topographically excited vertically propagating tidal modes.